Supporting Information for

"The Ligand Unwrapping/Rewrapping Pathway that Exchanges Metals in S-acetylated, Hexacoordinate $N_2S_2O_2$ Complexes"

J. A. Denny, W. S. Foley, A. D. Todd, M. Y. Darensbourg

Table of Contents **Page**

Figure S1. Cyclic voltammogram of **Ni-1'-Ac$_2$** in MeCN at a scan rate of 100 mV/s. $E_{1/2}$ is given in the Figure as 0.686 V vs. Fc/Fc^+. 3

Figure S2. Cyclic voltammograms of **Ni-1'-Ac$_2$** in MeCN showing the event at 0.686 V vs. Fc/Fc^+ at different scan rates. The current ratio, i_{pc}/i_{pa}, is 0.86. 3

Figure S3. Cyclic voltammogram of **Co-1'-Ac$_2$** in MeCN at a scan rate of 100 mV/s. $E_{1/2}$ is given in the Figure as -0.240 V vs. Fc/Fc^+. 4

Figure S4. Packing diagram of **Co-1'-Ac$_2$•2MeOH** highlighting the typical H-bonding network between the complex and co-crystallized solvent molecules. 4

Table S1. Molar absorptivity values used to calculate equilibrium values in H_2O. 5

Chart S1. Equations used to calculate equilibrium constants for metal exchange reactions. 6

Figure S5. UV-Vis monitoring in MeOH of the $Cu(NO_3)_2$/**Zn-1'-Ac$_2$** transmetallation reaction with the molar ratio of reactants 50:1, respectively. Reaction followed the band at 607 nm corresponding to appearance of **[Cu-1'-Ac$_2$]$_2$**. Time of injection corresponds to the spike in the spectra from the baseline where only spectroscopically silent Zn^{2+} was present. 7

Figure S6. UV-Vis spectral traces in MeOH for the reaction of a ten-fold excess of Ni^{2+} with **Co-1'-Ac$_2$** at ambient temperature, ca. 22 °C. The blue line corresponds to the spectra at the time of mixing and the orange line at completion, over the course of approximately 20 mins, following which time no further changes were observed. 8

Figure S7. Plot of k_{obs} vs. $[Ni^{2+}]$ at 298 K for the formation of **Ni-1'-Ac$_2$**. The R^2 value is 0.996. 9

Figure S8. Natural log plots of absorbance data vs. time for the formation of **Ni-1'-Ac$_2$** at various temperatures from the reaction of **Co-1'-Ac$_2$** and excess Ni(NO$_3$)$_2$.All best-fit lines have an R^2 value of >0.99. 9

Figure S9. Spectra and table of FT-IR values for **M-1'-Ac$_2$** complexes in CH_2Cl_2. 10

Figure S10. Arrhenius plot of the reaction of Co-1'-Ac2 and 25x Ni(NO3)2 in MeOH, which shows an activation energy of 16.3 kcal/mol. 10

Full Experimental Details 11

Figure S11. X-ray structure for **[Ni-1'-AA$_2$][I]$_2$** with thermal ellipsoids shown at 50% probability. Hydrogen atoms, solvent, and counter ions have been removed for clarity. 13

Figure S12. X-ray structure for **Fe-1'-Ac$_2$** with thermal ellipsoids shown at 50% probability. Hydrogen atoms and solvent have been removed for clarity. 14

Figure S13. X-ray structure for **Co-1'-Ac$_2$** with thermal ellipsoids shown at 50% probability. Hydrogen atoms and solvent have been removed for clarity. 15

Figure S14. X-ray structure for **[Cu-1'-Ac$_2$]$_2$** with thermal ellipsoids shown at 50% probability. Hydrogen atoms and solvent have been removed for clarity. 16

Figure S15. X-ray structure for **(bme-dach)(CH$_2$OH)$_2$** with thermal ellipsoids shown at 50% probability. Hydrogen atoms have been removed for clarity. 17

Table S2. Crystal table for **[Ni-1'-AA$_2$][I]$_2$**. 18

Table S3. Crystal table for **Co-1'-Ac$_2$**. 19

Table S4. Crystal table for **Fe-1'-Ac$_2$**. 20

Table S5. Crystal table for **[Cu-1'-Ac$_2$]$_2$**. 21

Table S6. Crystal table for (bme-dach)(CH_2OH)$_2$. 22

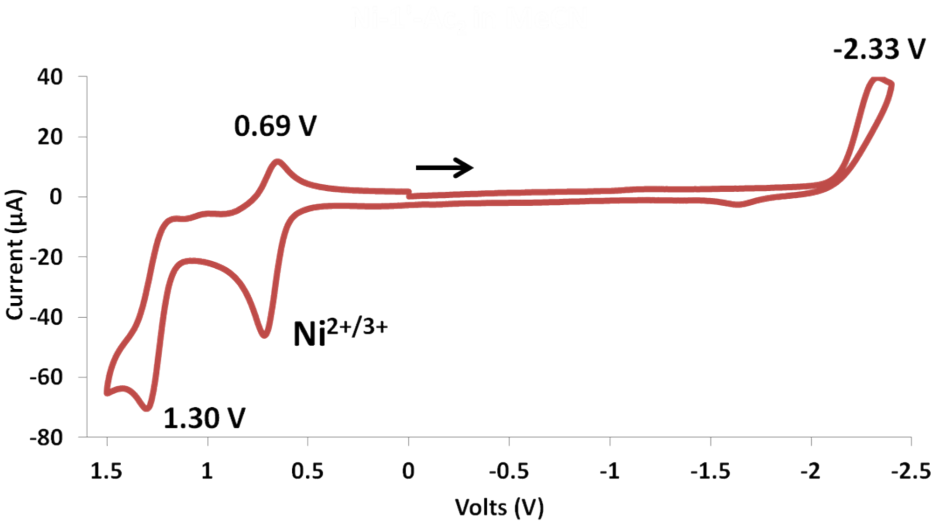

Figure S1. Cyclic voltammogram of **Ni-1’-Ac$_2$** in MeCN at a scan rate of 100 mV/s. $E_{1/2}$ is given in the Figure as 0.686 V vs. Fc/Fc$^+$.

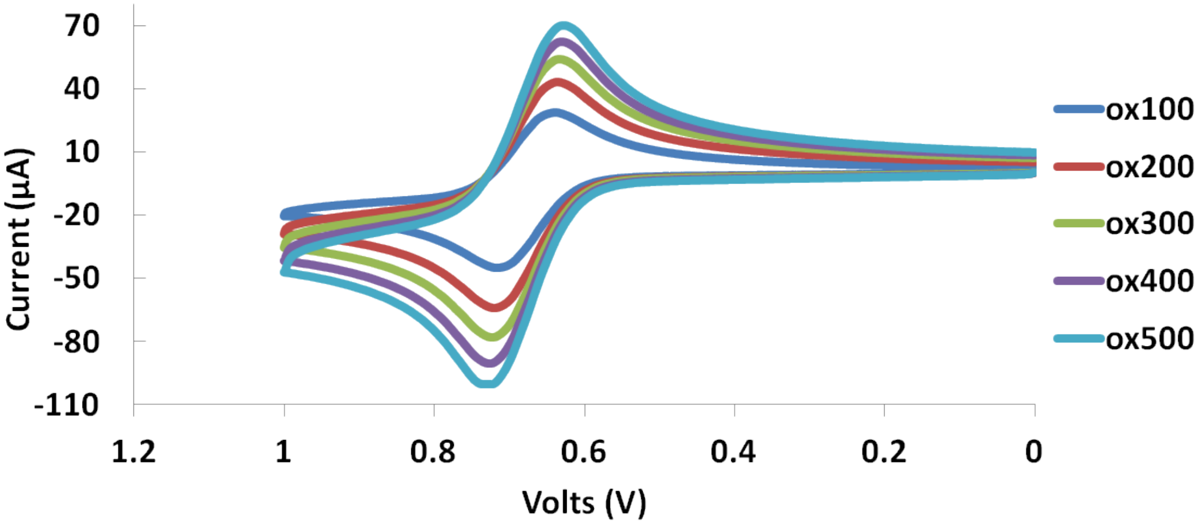

Figure S2. Cyclic voltammograms of **Ni-1’-Ac$_2$** in MeCN showing the event at 0.686 V vs. Fc/Fc$^+$ at different scan rates. The current ratio, i_{pc}/i_{pa}, is 0.86.

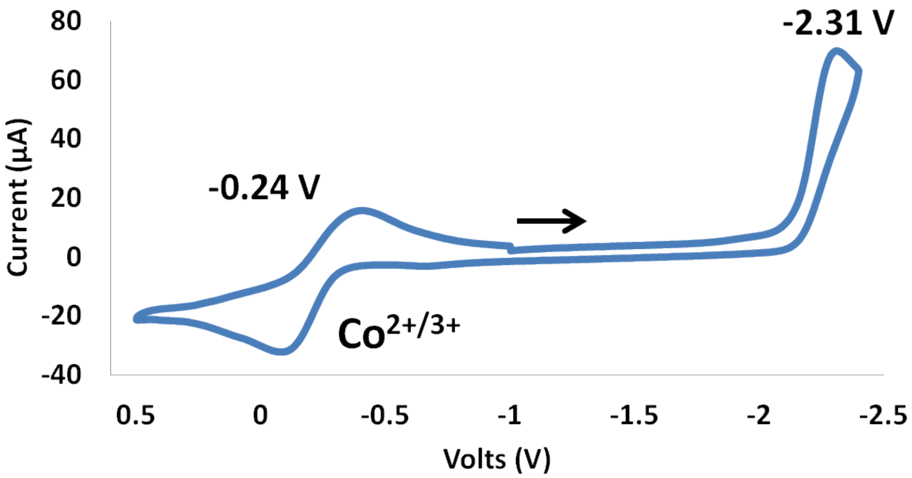

Figure S3. Cyclic voltammogram of **Co-1'-Ac$_2$** in MeCN at a scan rate of 100 mV/s. $E_{1/2}$ is given in the Figure as -0.240 V vs. Fc/Fc$^+$.

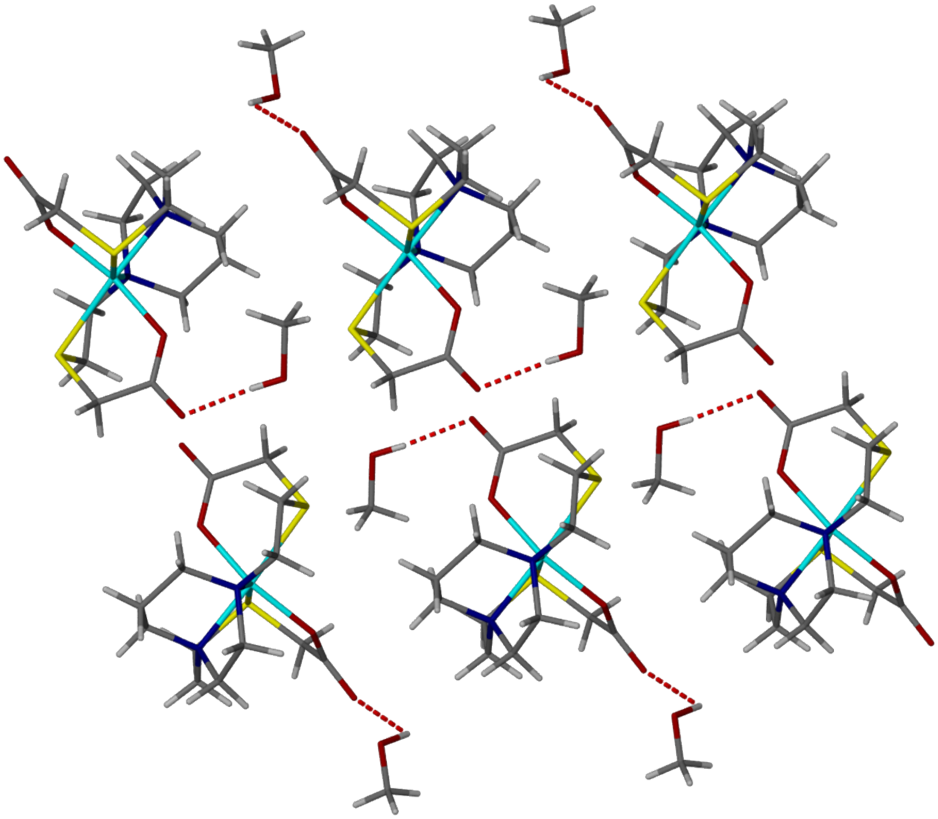

Figure S4. Packing diagram of **Co-1'-Ac$_2$•2MeOH** highlighting the typical H-bonding network between the complex and co-crystallized solvent molecules.

Table S1. Molar absorptivity values (ε, $M^{-1}cm^{-1}$) used to calculate equilibrium values in H_2O.

	359 nm	**497 nm**	**527 nm**	**564 nm**	**575 nm**
Co-1’-Ac_2	------	25.3	25.8	22.0	18.9
Ni-1’-Ac_2	27.5	-----	-----	-----	23.0
$Co(NO_3)_2$	-----	5.91	6.79	2.39	1.39
$Ni(NO_3)_2$	0.725	-----	-----	-----	0.254

Chart S1. Equations used to calculate equilibrium constants for metal exchange reactions.

$$A_1 = \varepsilon_1 * c_1$$

$$A_2 = \varepsilon_2 * c_2$$

$$A_1 + A_2 = A_{total}$$

$$\varepsilon_1 * c_1 + \varepsilon_2 * c_2 = A_{total}$$

$$c_1 = \frac{mol\ Co(NO_3)_2}{V_{total}}$$

$$c_2 = \frac{mol\ Co1'Ac_2}{V_{total}}$$

$$x + y = initial$$

$$\varepsilon_1 * \frac{x}{V_{total}} + \varepsilon_2 * \frac{initial - x}{V_{total}} = A_{total}$$

$$mol\ Ni(NO_3)_2 + mol\ Ni1'Ac_2 = mol\ initial\ Ni(NO_3)_2 = Z$$

$$mol\ Co(NO_3)_2 + mol\ Co1'Ac_2 = mol\ initial\ Co1'Ac_2 = Z$$

$$mol\ Co1'Ac_2 + mol\ Ni1'Ac_2 = mol\ initial\ mol\ Co1'Ac_2 = Z$$

$$mol\ Co(NO_3)_2 + mol\ Co1'Ac_2 = mol\ Co1'Ac_2 + mol\ Ni1'Ac_2$$

$$K = \frac{[Ni1'Ac_2][Co(NO_3)_2]}{[Co1'Ac_2][Ni(NO_3)_2]} = \frac{[Ni1'Ac_2][Ni1'Ac_2]}{[Co1'Ac_2][Ni(NO_3)_2]} = \frac{[Ni1'Ac_2][Ni1'Ac_2]}{[Z - Ni1'Ac_2][Z - Ni1'Ac_2]}$$

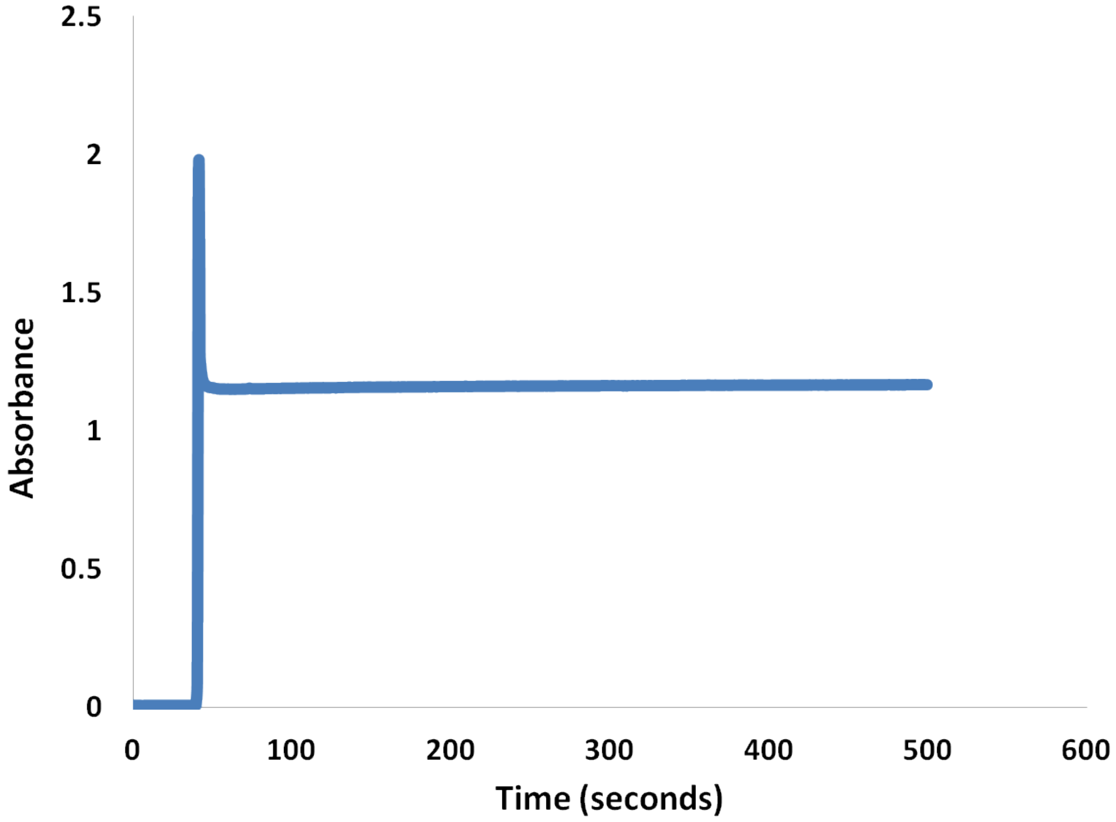

Figure S5. UV-Vis monitoring in MeOH of the $Cu(NO_3)_2$/**Zn-1’-Ac$_2$** transmetallation reaction with the molar ratio of reactants 50:1, respectively. Reaction followed the band at 607 nm corresponding to appearance of **[Cu-1’-Ac$_2$]$_2$**. Time of injection corresponds to the spike in the spectra from the baseline where only spectroscopically silent Zn^{2+} was present.

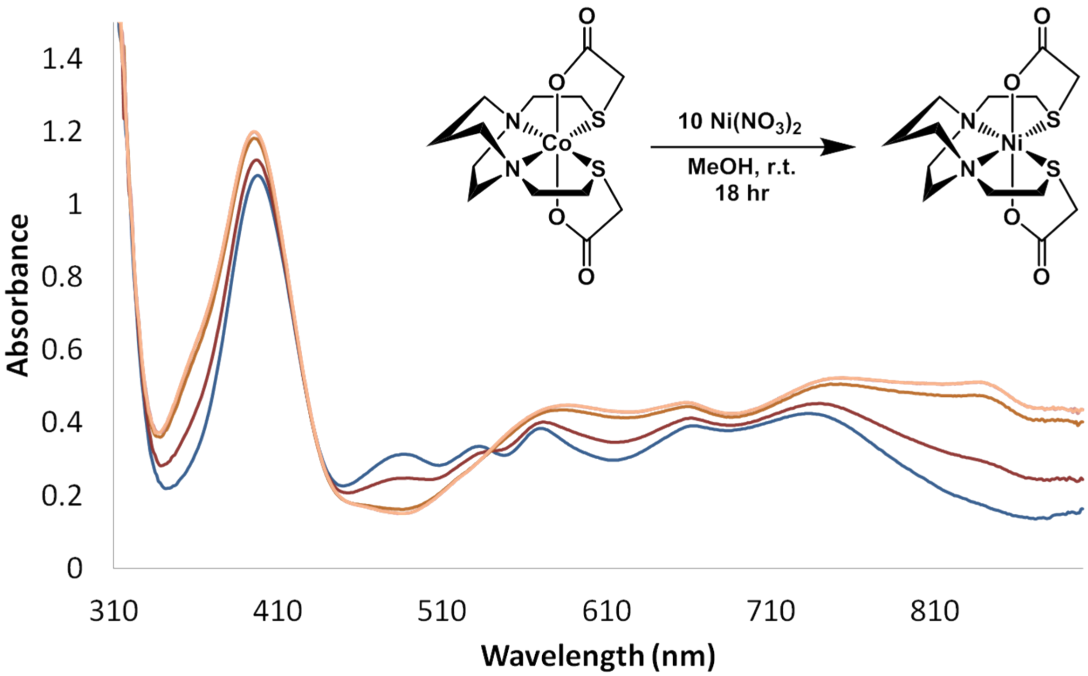

Figure S6. UV-Vis spectral traces in MeOH for the reaction of a ten-fold excess of Ni^{2+} with **Co-1'-Ac$_2$** at ambient temperature, ca. 22 °C. The blue line corresponds to the spectra at the time of mixing and the orange line at completion, over the course of approximately 20 mins, following which time no further changes were observed.

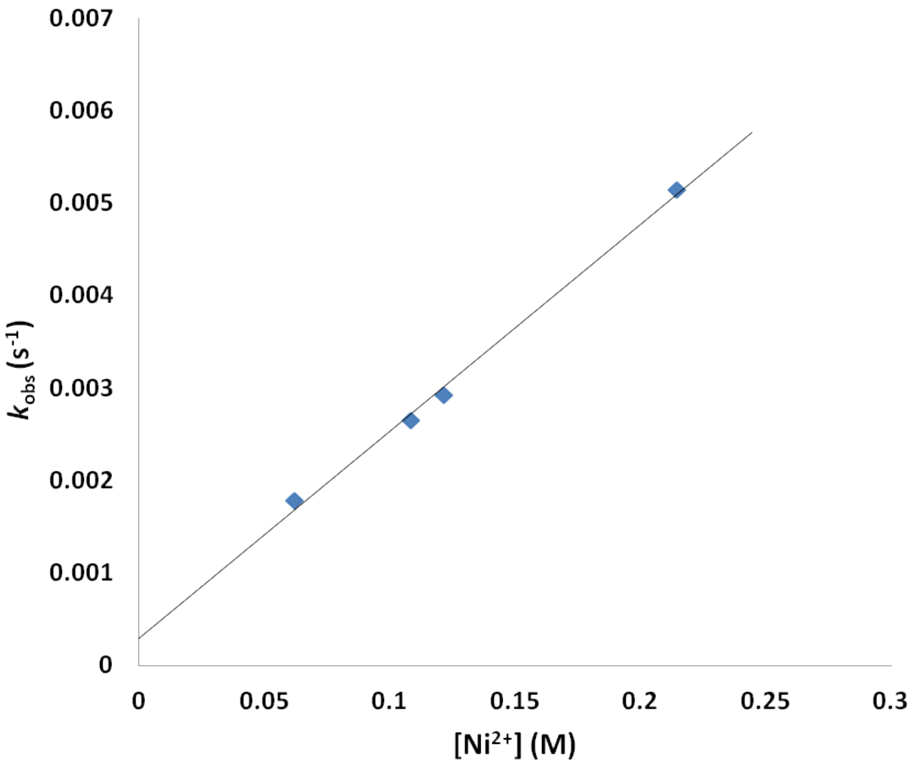

Figure S7. Plot of k_{obs} vs. $[Ni^{2+}]$ at 298 K for the formation of **Ni-1'-Ac$_2$**. The R^2 value is 0.996.

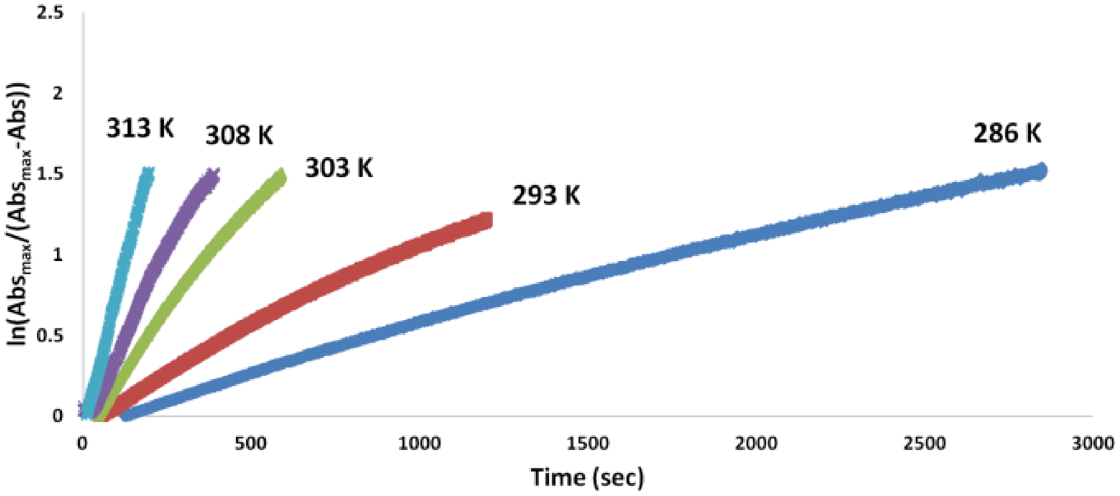

Figure S8. Natural log plots of absorbance data vs. time for the formation of **Ni-1'-Ac$_2$** at various temperatures from the reaction of **Co-1'-Ac$_2$** and excess $Ni(NO_3)_2$.All best-fit lines have an R^2 value of >0.99.

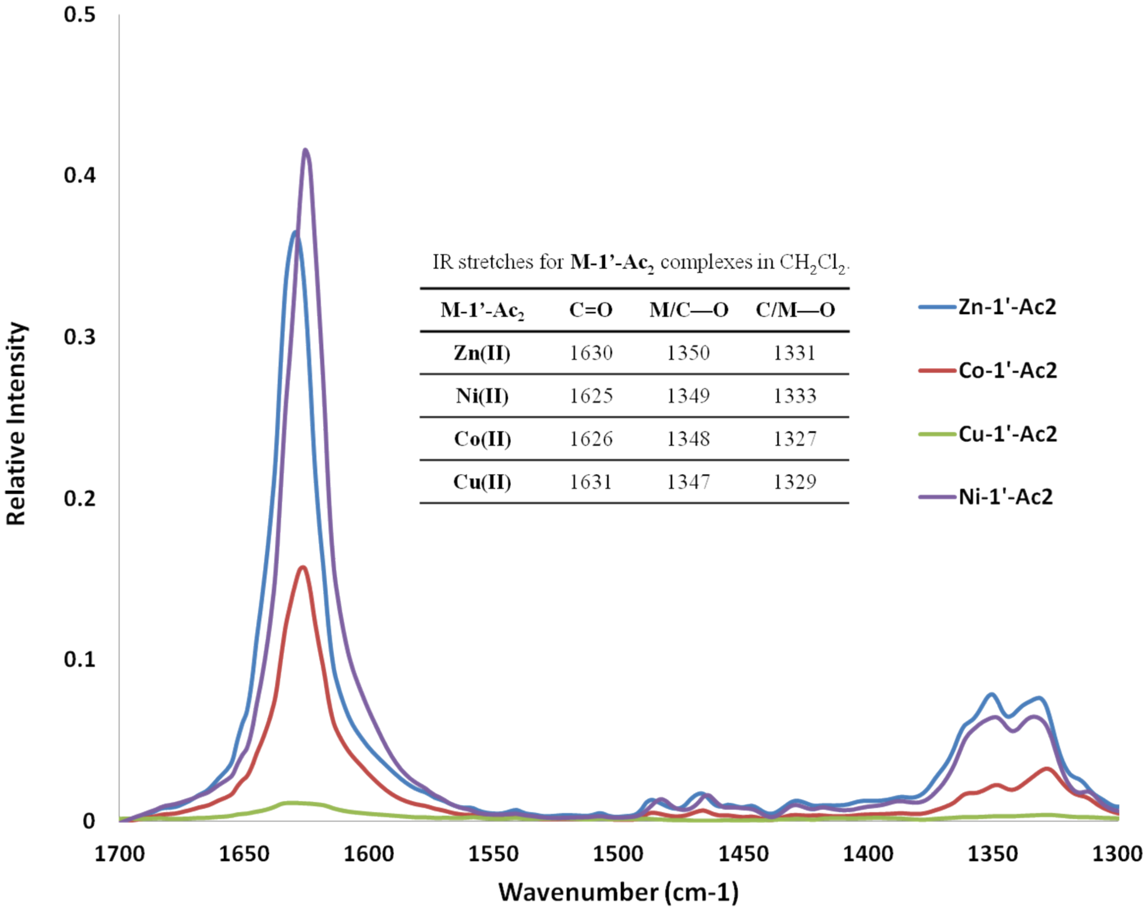

IR stretches for **M-1'-Ac$_2$** complexes in CH$_2$Cl$_2$.

M-1'-Ac$_2$	C=O	M/C—O	C/M—O
Zn(II)	1630	1350	1331
Ni(II)	1625	1349	1333
Co(II)	1626	1348	1327
Cu(II)	1631	1347	1329

Figure S9. Spectra and table of FT-IR values for **M-1'-Ac$_2$** complexes in CH$_2$Cl$_2$.

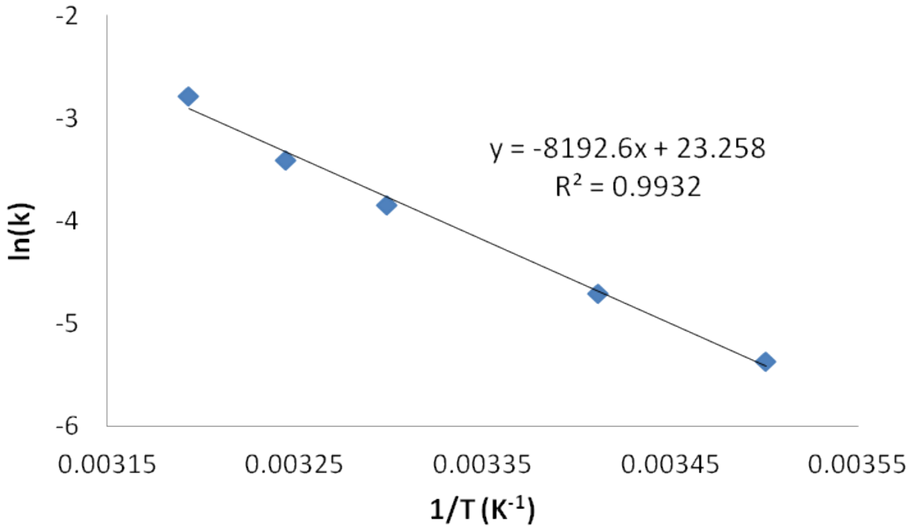

Figure S10. Arrhenius plot of the reaction of **Co-1'-Ac$_2$** and 25x Ni(NO$_3$)$_2$ in MeOH, which shows an activation energy of 16.3 kcal/mol.

Full Experimental Details

1,4-diazacycloheptane-1,4-diylbis(3-thiapentanoic) cobalt(II), Co-1'-Ac$_2$.

CoN$_2$S$_2$ Templated Synthesis. A sample of **[Co-1']$_2$** (0.50 g, 0.90 mmol) within a 250 mL Schlenk flask, was degassed prior to the addition of 50 mL of dry MeOH, producing a green solution. Sodium iodoacetate, Na$^+$IAc$^-$, (0.84 g, 4.0 mmol) in 40 mL dry MeOH, was added via cannula to the stirring **[Co-1']$_2$** solution. The solution became a dark red/brown and stirring was continued for 24 h; the solvent was reduced in vacuo and the mixture was filtered to remove any NaI formed. The filtrate was chromatographed on a silica gel column (3 x 20 cm) using a 1:1 MeOH:MeCN solvent mixture as eluent. An initial band of yellow material was discarded and the magenta product, with an R$_f$ value of 0.45, was collected. The solvent was removed in vacuo, and precipitation of a powder forced with addition of ether. The product was collected by filtration, washed 3x with ether, and dried in vacuo yielding 0.40 g (0.88 mmol, 98%) of **Co-1'-Ac$_2$•2MeOH** solid. ESI-mass spectrum in CH_3OH: $[CoN_2S_2O_4C_{13}H_{22} + Na^+]^+$ m/z = 416 (27%). UV-Vis (CH_3OH): λ_{max}, nm (ε, $M^{-1}cm^{-1}$) = 570 (29), 537 (28), 487 (30), 279 (408) nm. IR (in CH_2Cl_2, cm^{-1}): 1627 (vs, sharp), 1348 (m), 1329 (m). Cyclic Voltammetry: $E_{1/2}$ = -240 mV vs. Fc/Fc$^+$ in MeCN assigned to the Co^{III}/Co^{II} couple. Magnetic moment, Guoy Balance: 4.79 B.M. Elem. Anal. Calc'd for **Co-1'-Ac$_2$•**2MeOH, $CoN_2S_2O_6C_{15}H_{30}$ (found): C: 39.38 (39.09), H: 6.61 (6.03), N: 6.12 (6.42).

Cobalt Ion Exchange into Zn-1'-Ac$_2$. To a 0.20 g, 0.51 mmol, sample of **Zn-1'-Ac$_2$**, 75 mL of dry degassed MeOH was added, producing a clear colorless solution to which was added 0.15 g, 0.51 mmol of $Co(NO_3)_2$ as a light pink solution in 25 mL dry MeOH. The mixture was stirred for 24 h. The solid magenta product was isolated as above to yield 0.14 g (0.37 mmol, 72%); characterization matched above results.

Hexadentate N$_2$S$_2$O$_2$ Ligand Synthesis Followed by Addition of Co(NO$_3$)$_2$. The H$_2$bme-dach ligand (0.50 g, 2.3 mmol) was placed in a 500 mL Schlenk flask under Ar along with 50 mL of dry MeOH. To this flask Na$^+$IAc$^-$ (1.0 g, 5.0 mmol) in 50 mL dry MeOH was added. The pale yellow solution was magnetically stirred for 18 h before it was used *in situ*. To the stirring acetylated bme-dach ligand solution, $Co(NO_3)_2$ (0.66 g, 2.3 mmol) was added as a clear pink solution in 50 mL of dry MeOH whereupon a magenta color developed. The solution volume was partially reduced in vacuo before filtering to remove Na$^+$ salts formed during the reaction. Addition of Et_2O resulted in precipitation of a magenta solid, which was isolated by filtration. This powder was redissolved in MeOH and chromatographed through a silica gel column with MeOH as the eluent yielding 0.36 g (0.92 mmol, 40%). The properties of this product matched those from the templated synthetic route.

1,4-diazacycloheptane-1,4-diylbis(3-thiapentanoic) copper(II), [Cu-1'-Ac$_2$]$_2$.

CuN$_2$S$_2$ Templated Synthesis. As a monomer Cu-1' is not known, a templated synthesis similar to that used with **Ni-1'** or **[Co-1']$_2$** was not attempted.

Copper Ion Exchange into Zn-1'-Ac$_2$. A 100 mL Schlenk flask was charged with a sample of **Zn-1'-Ac$_2$** (0.10 g, 0.25 mmol) and degassed prior to the addition of 25 mL of dry MeOH, producing a clear colorless solution. Copper nitrate, $Cu(NO_3)_2$, (0.059 g, 0.25 mmol) in 25 mL dry MeOH was added via cannula to the stirring **Zn-1'-Ac$_2$** solution. The solution developed a very intense blue color and stirring was continued for 24 h. The solvent was reduced in vacuo, and then Et_2O was added to force precipitation of a blue powder which was collected by filtration. Under moisture-excluding conditions the product, washed 3x with Et_2O, was redissolved in MeOH and chromatographed through a silica gel column (3 x 20 cm) using MeOH as the eluent. The material with an R_f value of 0.25 was collected as the desired product, the solvent was reduced in vacuo, and precipitation forced with addition of Et_2O. The sticky blue product was collected by anerobic filtration, redissolved, precipitated, and washed until a blue powder could be isolated. This powder was further dried in vacuo yielding 0.030 g (0.076 mmol, 30%) of **[Cu-1'-Ac₂]₂** solid. ESI-mass spectrum in CH_3OH: $[CuN_2S_2O_4C_{13}H_{22} + H^+]^+$ m/z = 398. UV-Vis (CH_3OH): λ_{max}, nm (ε, $M^{-1}cm^{-1}$) = 607 (202), 348 (2660), 287 (1560) nm. IR (in CH_2Cl_2, cm^{-1}): 1631 (vs, sharp), 1347 (m), 1329 (m). $E_{1/2}$ = -360 mV vs. Fc/Fc^+ in CH_2Cl_2 for the Cu^{II}/Cu^{I} couple. Magnetic moment, Evans Method: 1.46 B.M. Elem. Anal. Calc'd for Cu-1'-Ac_2•H_2O, $CuN_2S_2O_5C_{13}H_{24}$ (found): C: 37.53 (37.04), H: 5.81 (5.76), N: 6.73 (6.64).

Hexadentate $N_2S_2O_2$ Ligand Synthesis Followed by Addition of $Cu(NO_3)_2$. The H_2bme-dach ligand (0.23 g, 1.0 mmol) was placed in a 100 mL Schlenk flask and 10 mL of dry MeOH was added. To this flask, Na^+IAc^- (0.45 g, 2.2 mmol) in 15 mL dry MeOH was added. The pale yellow solution was magnetically stirred for 18 h prior to the addition of $Cu(NO_3)_2$ (0.25 g, 1.0 mmol) in 20 mL of a degassed 50/50 $MeOH/H_2O$ mixture was added to the ligand solution, whereupon a rich blue solution developed along with an unknown green/brown precipitate. After stirring overnight, the solution was filtered anerobically through Celite. The filtrate volume was partially reduced in vacuo before Et_2O addition precipitated a blue powder. The powder was redissolved in MeOH and chromatographed through a silica gel column (3 x 20 cm) with MeOH as the eluent. The blue fractions were combined and the solvent was reduced, followed by precipitation with Et_2O to yield a blue powder. The powder was washed with Et_2O and dried in vacuo to yield 0.096 g (0.24 mmol, 24%) **[Cu-1'-Ac₂]₂** solid. The product had identical properties as described above.

1,4-diazacycloheptane-1,4-diylbis(3-thiapentanoic) iron(II), Fe-1'-Ac₂.

FeN_2S_2 Templated Synthesis. A sample of **[Fe-1']₂** (0.250 g, 0.456 mmol) within a 250 mL Schlenk flask, was degassed prior to the addition of 75 mL of dry MeOH, producing a brown solution. Sodium iodoacetate, Na^+IAc^-, (0.475 g, 2.28 mmol) in 30 mL dry MeOH was added via cannula to the stirring **[Fe-1']₂** solution. The solution became a cloudy yellow/brown and was allowed to react overnight; solvent was reduced in vacuo, and then filtered to remove NaI formed. The solution was purified by silica column chromatography using MeOH as the eluent, the second yellow band was collected. The volume was reduced and product precipitated upon ether addition. The powder was collected by anerobic filtration, washed 3x with ether, and dried in vacuo to yield 0.259 g (0.659 mmol 72%) **Fe-1'-Ac₂** solid. ESI-mass spectrum in CH_3OH: $[FeN_2S_2O_4C_{13}H_{22} + H^+]^+$ m/z = 391. UV-Vis (CH_3OH): λ_{max}, nm (ε, $M^{-1}cm^{-1}$) = 346 (2660), 280 (1560) nm. IR (in CH_2Cl_2, cm^{-1}): 1631 (vs, sharp), 1348 (m), 1327 (m).

Hexadentate $N_2S_2O_2$ Ligand Synthesis Followed by Addition of $Fe(NO_3)_2$. The H_2bme-dach (0.250 g, 1.13 mmol) was placed in a 250 mL Schlenk flask and 20 mL of dry MeOH was added. To this flask, Na^+IAc^- (0.520 g, 2.50 mmol) in 20 mL dry MeOH was added. The pale yellow solution was magnetically stirred for 18 h before it was used *in situ*. Then $Fe(NO_3)_2$ (0.317 g, 1.13 mmol), in 25 mL of dry MeOH, was added to the ligand solution, whereupon a yellow solution and an off-white precipitate developed. After overnight stirring the solution was anerobically filtered and solvent was reduced in vacuo. The solution was purified as above in the templated synthesis to yield 0.294 g (0.753 mmol 66%) **Fe-1'-Ac₂** solid. The product had identical characterization as above.

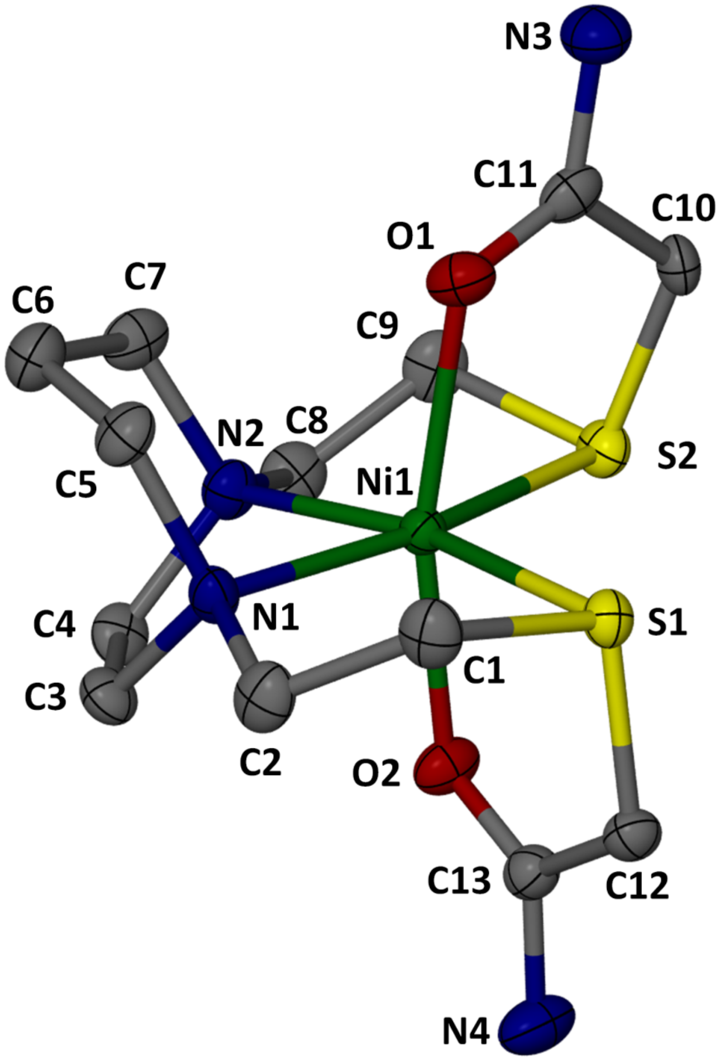

Figure S11. X-ray structure for **[Ni-1’-AA$_2$][I]$_2$** with thermal ellipsoids shown at 50% probability. Hydrogen atoms, solvent, and counter ions have been removed for clarity.

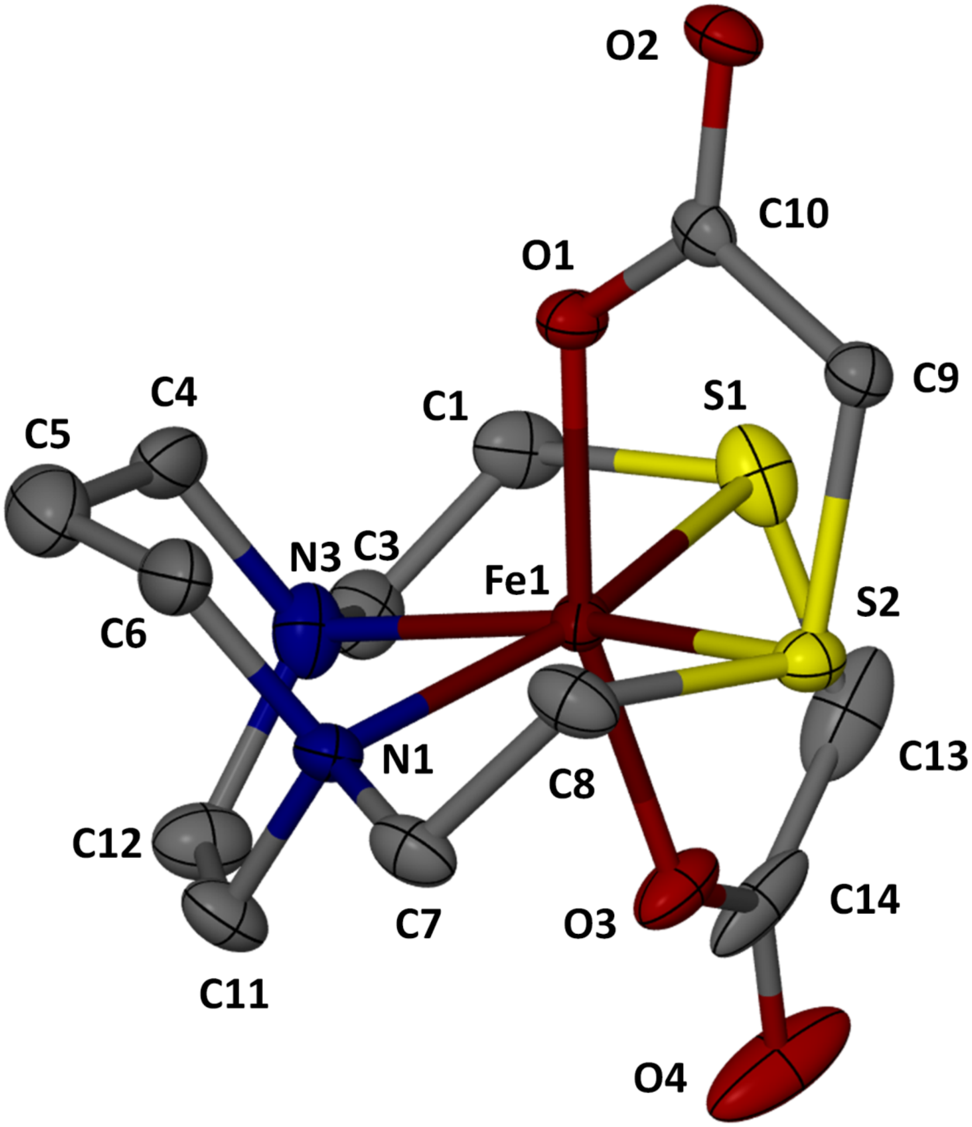

Figure S12. X-ray structure for **Fe-1’-Ac$_2$** with thermal ellipsoids shown at 50% probability. Hydrogen atoms and solvent have been removed for clarity.

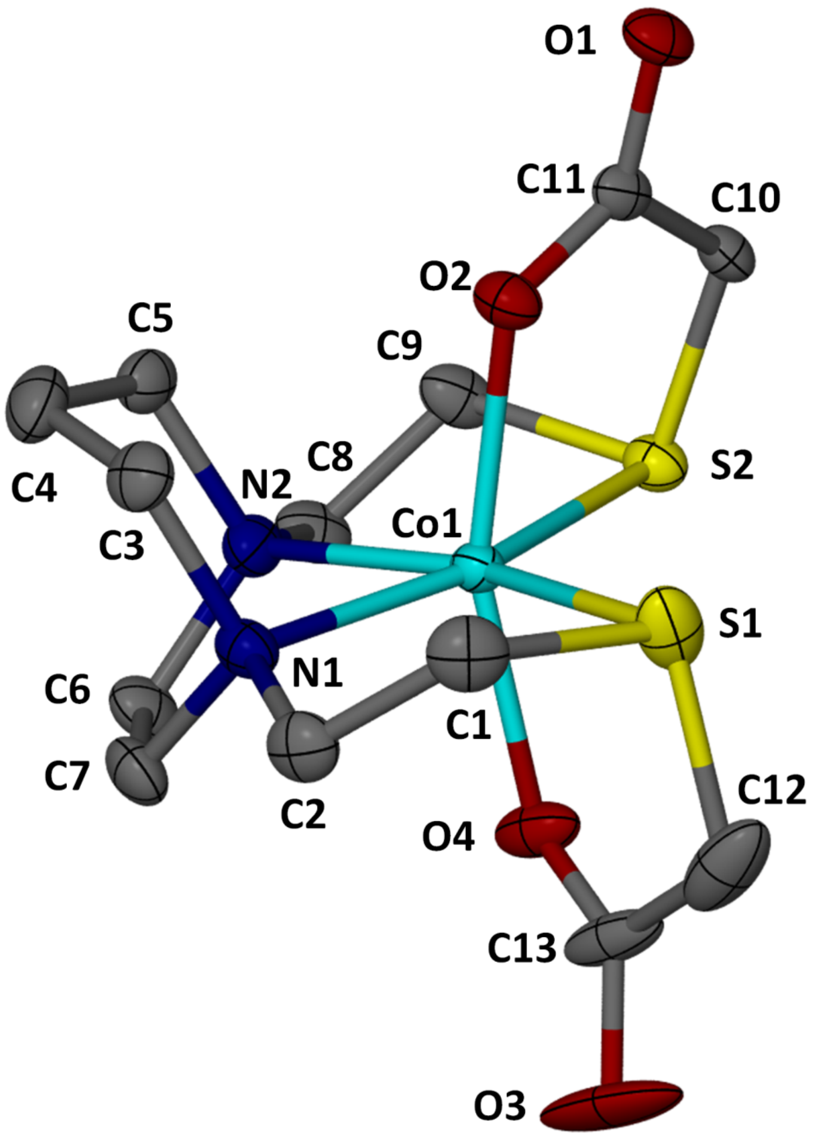

Figure S13. X-ray structure for **Co-1'-Ac$_2$** with thermal ellipsoids shown at 50% probability. Hydrogen atoms and solvent have been removed for clarity

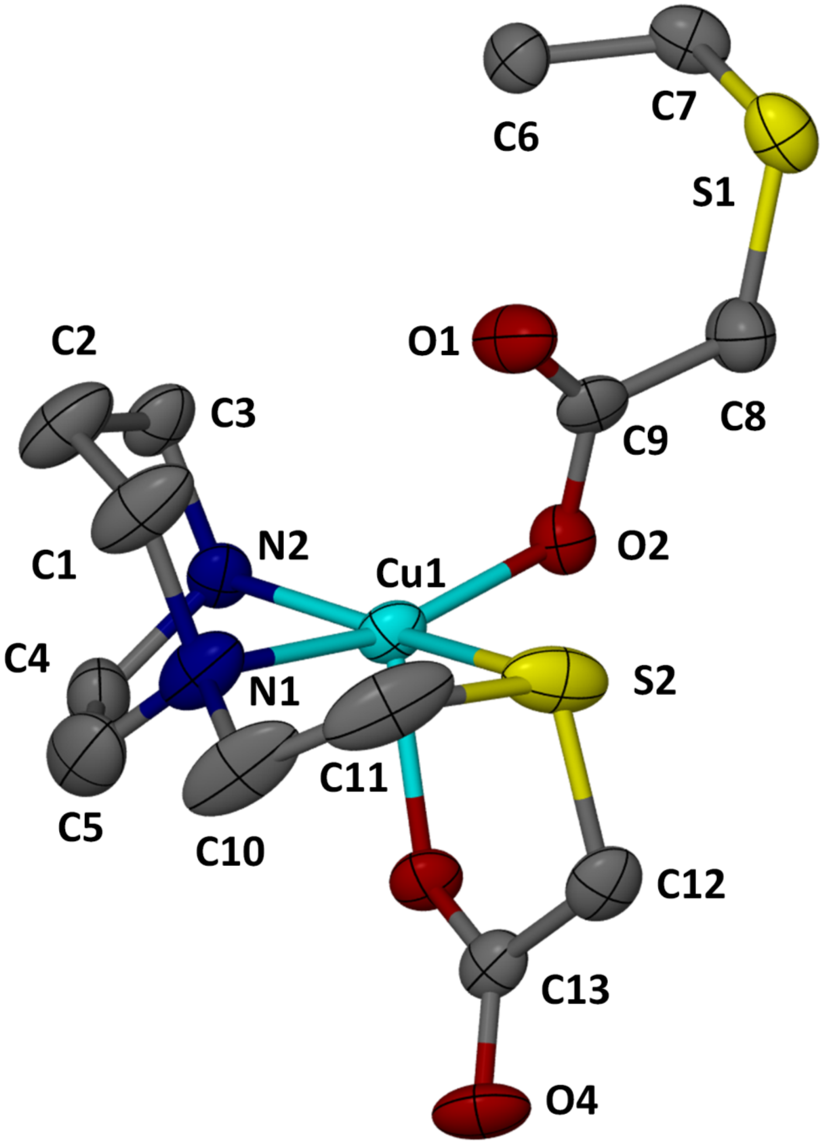

Figure S14. X-ray structure for **[Cu-1’-Ac$_2$]$_2$** with thermal ellipsoids shown at 50% probability. Hydrogen atoms and solvent have been removed for clarity.

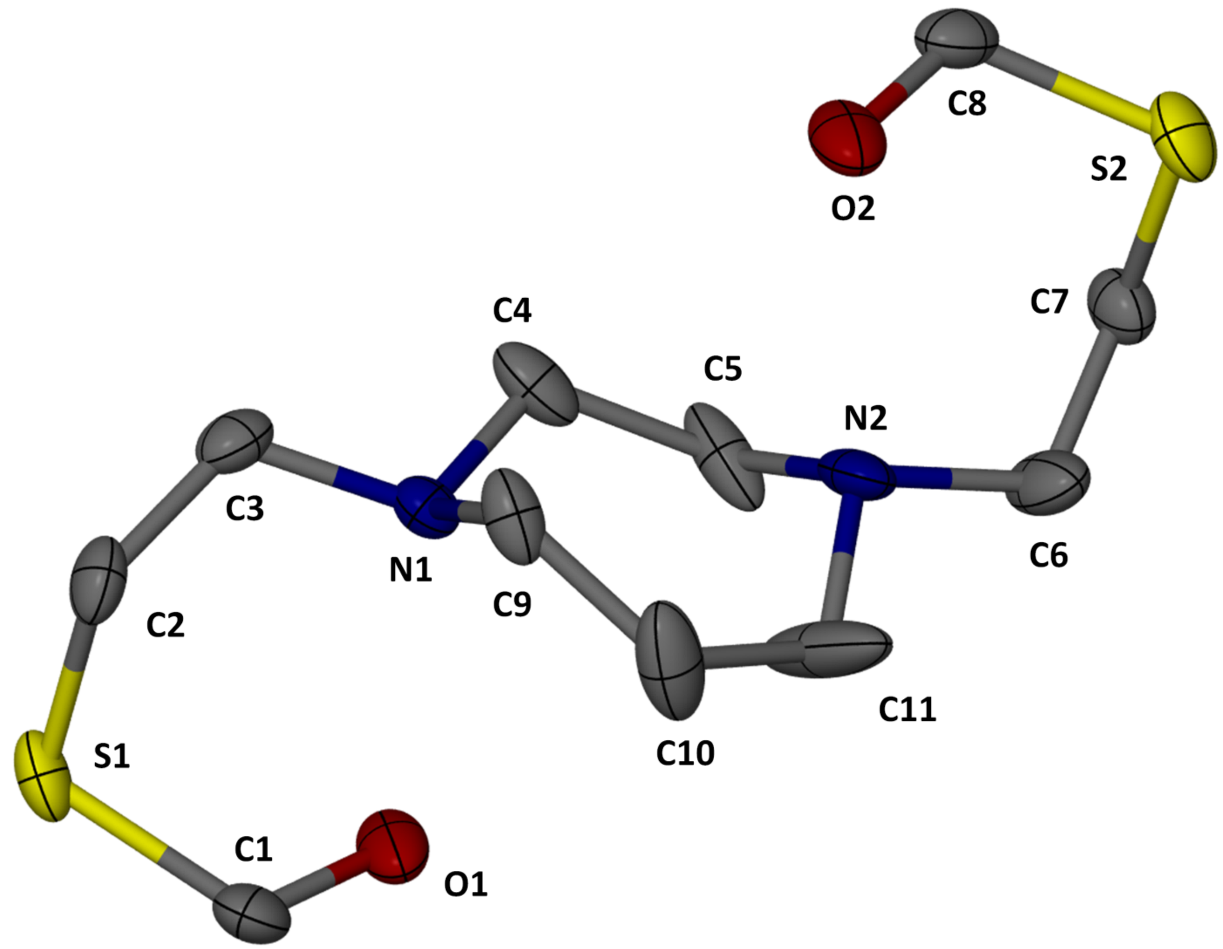

Figure S15. X-ray structure for **(bme-dach)(CH_2OH)$_2$** with thermal ellipsoids shown at 50% probability. Hydrogen atoms have been removed for clarity.

Table S2. Crystal data and structure refinement for **Ni-1'-AA$_2$**.

Identification code	NiAA2	
Empirical formula	C15 H34 I2 N4 Ni O4 S2	
Formula weight	711.09	
Temperature	150(2) K	
Wavelength	0.71073 Å	
Crystal system	Triclinic	
Space group	P -1	
Unit cell dimensions	a = 10.141(3) Å	α= 86.263(4)°.
	b = 11.619(4) Å	β= 69.710(3)°.
	c = 11.643(4) Å	γ = 76.551(4)°.
Volume	1251.2(7) Å^3	
Z	2	
Density (calculated)	1.887 Mg/m^3	
Absorption coefficient	3.436 mm^{-1}	
F(000)	700	
Crystal size	0.29 x 0.15 x 0.08 mm^3	
Theta range for data collection	1.80 to 27.57°.	
Index ranges	-12<=h<=12, -15<=k<=15, -15<=l<=15	
Reflections collected	37396	
Independent reflections	5640 [R(int) = 0.0548]	
Completeness to theta = 27.57°	97.5 %	
Absorption correction	Semi-empirical from equivalents	
Max. and min. transmission	0.7706 and 0.4357	
Refinement method	Full-matrix least-squares on F^2	
Data / restraints / parameters	5640 / 59 / 336	
Goodness-of-fit on F^2	1.047	
Final R indices [I>2sigma(I)]	R1 = 0.0365, wR2 = 0.0901	
R indices (all data)	R1 = 0.0479, wR2 = 0.0955	
Largest diff. peak and hole	1.089 and -1.166 e.Å^{-3}	

Table S3. Crystal data and structure refinement for **Co-1'-Ac$_2$**.

Identification code	CoAc2	
Empirical formula	C15 H29 Co N2 O6 S2	
Formula weight	456.45	
Temperature	110(2) K	
Wavelength	0.71073 Å	
Crystal system	Triclinic	
Space group	P -1	
Unit cell dimensions	a = 7.5419(17) Å	α= 78.174(3)°.
	b = 8.0477(18) Å	β= 82.069(3)°.
	c = 16.687(4) Å	γ = 86.421(3)°.
Volume	981.3(4) Å^3	
Z	2	
Density (calculated)	1.545 Mg/m^3	
Absorption coefficient	1.121 mm^{-1}	
F(000)	480	
Crystal size	0.34 x 0.14 x 0.14 mm^3	
Theta range for data collection	2.51 to 27.75°.	
Index ranges	-9<=h<=9, -10<=k<=10, -21<=l<=21	
Reflections collected	32449	
Independent reflections	4580 [R(int) = 0.0315]	
Completeness to theta = 27.75°	99.1 %	
Absorption correction	Semi-empirical from equivalents	
Max. and min. transmission	0.8589 and 0.7018	
Refinement method	Full-matrix least-squares on F^2	
Data / restraints / parameters	4580 / 30 / 289	
Goodness-of-fit on F^2	1.119	
Final R indices [I>2sigma(I)]	R1 = 0.0379, wR2 = 0.0851	
R indices (all data)	R1 = 0.0496, wR2 = 0.0930	
Largest diff. peak and hole	0.829 and -0.519 e.Å^{-3}	

Table S4. Crystal data and structure refinement for **Fe-1'-Ac$_2$**.

Identification code	FeAc2	
Empirical formula	C15 H28 Fe N2 O6 S2	
Formula weight	452.36	
Temperature	110(2) K	
Wavelength	0.71073 Å	
Crystal system	Triclinic	
Space group	P -1	
Unit cell dimensions	a = 7.486(7) Å	α= 78.165(13)°.
	b = 8.040(8) Å	β= 82.235(13)°.
	c = 16.740(16) Å	γ = 86.603(13)°.
Volume	976.5(16) Å^3	
Z	2	
Density (calculated)	1.539 Mg/m^3	
Absorption coefficient	1.020 mm^{-1}	
F(000)	476	
Crystal size	0.10 x 0.10 x 0.10 mm^3	
Theta range for data collection	1.25 to 28.81°.	
Index ranges	-10<=h<=9, -10<=k<=10, -22<=l<=22	
Reflections collected	10836	
Independent reflections	4570 [R(int) = 0.0873]	
Completeness to theta = 28.81°	89.4 %	
Absorption correction	Semi-empirical from equivalents	
Max. and min. transmission	0.9049 and 0.9049	
Refinement method	Full-matrix least-squares on F^2	
Data / restraints / parameters	4570 / 0 / 237	
Goodness-of-fit on F^2	1.126	
Final R indices [I>2sigma(I)]	R1 = 0.0576, wR2 = 0.1555	
R indices (all data)	R1 = 0.0814, wR2 = 0.1647	
Largest diff. peak and hole	1.225 and -0.970 e.Å^{-3}	

Table S5. Crystal data and structure refinement for **[Cu-1'-Ac$_2$]$_2$**.

Identification code	mono	
Empirical formula	C30 H56 Cu2 N4 O12 S4	
Formula weight	920.11	
Temperature	150(2) K	
Wavelength	0.71073 Å	
Crystal system	Monoclinic	
Space group	C 2/c	
Unit cell dimensions	a = 19.683(3) Å	α= 90°.
	b = 12.1661(19) Å	β= 106.346(3)°.
	c = 19.517(3) Å	γ = 90°.
Volume	4484.6(12) Å^3	
Z	4	
Density (calculated)	1.363 Mg/m^3	
Absorption coefficient	1.190 mm^{-1}	
F(000)	1928	
Crystal size	0.15 x 0.06 x 0.03 mm^3	
Theta range for data collection	1.99 to 21.89°.	
Index ranges	-20<=h<=20, -12<=k<=12, -20<=l<=20	
Reflections collected	46585	
Independent reflections	2566 [R(int) = 0.0753]	
Completeness to theta = 21.89°	94.5 %	
Absorption correction	Semi-empirical from equivalents	
Max. and min. transmission	0.9709 and 0.8417	
Refinement method	Full-matrix least-squares on F^2	
Data / restraints / parameters	2566 / 0 / 237	
Goodness-of-fit on F^2	1.108	
Final R indices [I>2sigma(I)]	R1 = 0.0418, wR2 = 0.0993	
R indices (all data)	R1 = 0.0627, wR2 = 0.1059	
Largest diff. peak and hole	0.400 and -0.302 e.Å^{-3}	

Table S6. Crystal data and structure refinement for (bme-dach)$(CH_2OH)_2$.

Identification code	e:_s~1~1	
Empirical formula	C11 H24 N2 O2 S2	
Formula weight	280.44	
Temperature	150(2) K	
Wavelength	0.71073 Å	
Crystal system	Monoclinic	
Space group	P 21/c	
Unit cell dimensions	a = 9.6252(8) Å	α= 90°.
	b = 12.3461(10) Å	β= 103.606(4)°.
	c = 12.2335(10) Å	γ = 90°.
Volume	1413.0(2) $Å^3$	
Z	4	
Density (calculated)	1.318 Mg/m^3	
Absorption coefficient	0.371 mm^{-1}	
F(000)	608	
Crystal size	0.10 x 0.10 x 0.10 mm^3	
Theta range for data collection	2.18 to 27.75°.	
Index ranges	-12<=h<=12, -16<=k<=16, -15<=l<=16	
Reflections collected	27616	
Independent reflections	3313 [R(int) = 0.0458]	
Completeness to theta = 27.75°	99.7 %	
Absorption correction	Semi-empirical from equivalents	
Max. and min. transmission	0.9639 and 0.9639	
Refinement method	Full-matrix least-squares on F^2	
Data / restraints / parameters	3313 / 0 / 162	
Goodness-of-fit on F^2	1.040	
Final R indices [I>2sigma(I)]	R1 = 0.0666, wR2 = 0.1657	
R indices (all data)	R1 = 0.0740, wR2 = 0.1731	
Largest diff. peak and hole	1.401 and -0.742 e.$Å^{-3}$	